Potential-Dependent Reconstruction at Ordered Au(100)-Aqueous Interfaces as Probed by Atomic-Resolution Scanning Tunneling Microscopy

Xiaoping Gao, Antoinette Hamelin,[a] and Michael J. Weaver
Department of Chemistry, Purdue University, West Lafayette, Indiana 47907
(Received 8 April 1991)

Detailed atomic-resolution images of ordered Au(100) surfaces in aqueous 0.1*M* $HClO_4$ as obtained by *in situ* scanning tunneling microscopy (STM) are reported as a function of electrode potential. Below ca. −0.25 V (versus saturated calomel electrode), the (1×1) surface reconstructs to form corrugated quasihexagonal domains. Multiple distinct, yet related, structures are formed that resemble those postulated from diffraction measurements. The reconstruction can be lifted by returning to 0.2 V. The results demonstrate the promise of atomic-resolution STM for examining reconstruction at ordered electrochemical surfaces.

PACS numbers: 68.45.−v, 61.16.Di

Elucidating the atomic structures formed upon reconstruction of ordered metal interfaces is a topic of major importance in surface science. Knowledge of such structures, and their sensitivity to system conditions, is crucial to our understanding of surface crystallographic effects in adsorption, catalysis, and so on. Almost all our experimental understanding so far has been obtained in ultrahigh-vacuum (UHV) environments, especially by means of low-energy electron diffraction (LEED) and allied techniques. Reconstruction has long been thought to occur at ordered metal-solution interfaces, based on conventional electrochemical measurements, especially for gold-aqueous systems [1]. Microscopic evidence for such phenomena on gold has been obtained more recently by means of emersion of the surface into UHV with subsequent LEED and related analyses [2]. The acquisition of reliable potential-dependent information on reconstruction, however, requires *in situ* techniques, i.e., those applicable directly to the metal-solution interface.

In situ approaches utilized recently to this end include second-harmonic generation (SHG) [3] and grazing-incidence x-ray diffraction [4], both at low-index gold-aqueous interfaces. While the latter technique, in particular, can provide detailed surface structural information, it is limited by the availability of high-intensity (synchrotron) x-ray sources. Scanning tunneling microscopy (STM) is arguably the most promising candidate for this purpose since it can yield direct (real-space) surface structures. While a number of *in situ* electrochemical STM studies have been reported recently, including several at gold interfaces [5–7], very few have achieved the *true* atomic resolution (i.e., identification of individual surface atoms) necessary for fundamental insight into surface reconstruction to be attained. Some recent reports, however, indicate that atomic-resolution STM images can be obtained for simple atomic and molecular adlayers at metal-solution interfaces [8–11].

We report here atomic-resolution STM images for a well-ordered Au(100) surface in aqueous 0.1*M* $HClO_4$ as a function of electrode potential. The results not only provide the first direct real-space observation of potential-induced surface reconstruction in an electrochemical system, but also provide detailed information on the atomic structures thus formed. The Au(100) system is of particular interest in this regard. Besides recent *in situ* studies at Au(100)-aqueous interfaces by SHG [3] and x-ray reflectance and diffraction [4], the Au(100)-UHV surface has been examined extensively by LEED [12] and other structural techniques, including STM [13–16]. The present findings allow some resolution of the various alternative structural models proposed previously for reconstructed Au(100) [12].

The Au(100) crystal (hemisphere, 5 mm diameter) was grown, cut, and polished at Laboratoire d'Electrochimie Interfaciale, CNRS, as outlined in the Appendix of Ref. [17]; the nominal orientation is within ±0.25°. The crystal was flame annealed immediately before each experiment, cooled in ultrapure water, and transferred to the STM cell protected by a drop of water. The open base of the Kel-F cell was sealed to the Au surface by set screws [9–11]. Most details of the *in situ* STM measurements have been noted previously [9,10,18]. The microscope is a commercial Nanoscope II instrument (Digital Instruments, Inc.) with a bipotentiostat for *in situ* electrochemical STM. The atomic-resolution STM images were obtained in the "constant-height" mode. The set-point current i_t was typically ca. 15 nA, and the bias voltage V_b was usually 5–10 mV. Variations in the electrode potential E were made with V_b held constant. The STM tips were made from 0.010-in. tungsten wire electrochemically etched in 1*M* KOH, and insulated with clear nail polish. The counterelectrode was a platinum wire, and the quasi reference electrode was a freshly electro-oxidized gold wire.

After assembling the STM cell with the freshly annealed crystal, aqueous 0.1*M* $HClO_4$ was added and an anodic-cathodic cyclic voltammogram (50 $mV s^{-1}$) recorded to check the surface state. A typical voltammogram is shown (solid trace) in Fig. 1. (When the solution was deaerated, the dashed component in Fig. 1 was observed.) Typically, the potential was returned to about 0.2 V versus saturated calomel electrode (SCE) after a voltammetric cycle; the STM images were unstable at substantially higher potentials, due to interference from

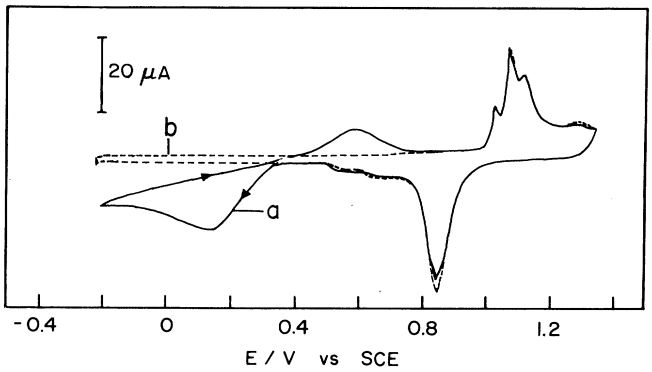

FIG. 1. Typical cyclic voltammogram (50 $mV s^{-1}$) for annealed Au(100) (area =0.50 cm^2) in deaerated 0.1M $HClO_4$ within STM cell. Dashed segment is that obtained without the presence of air.

Faradaic tip currents.

Figure 2(a) shows a 2D-Fourier-transform-filtered STM image obtained under these conditions, at 0.2 V versus SCE. A regular square-planar image with interatomic distances, 2.9 Å, appropriate for the (1×1) (unreconstructed) gold substrate can be discerned. [Note that the images shown here are uncorrected for thermal drift, accounting for the distortion from the actual square-planar lattice in Fig. 2(a); the interatomic distances, however, are usually accurate to within ca. 5%.] Large (at least 300 Å) (1×1) terraces could usually be observed. Such images are stable for at least 1 h at ca. 0–0.2 V versus SCE.

Adjusting the electrode potential to more negative values, in 0.1-V increments, yielded dramatic changes in the STM images. Initially, "waves" in the previously flat (1×1) terraces appeared. At −0.3 to −0.4 V, large regions of these terraces were transformed within a few minutes into corrugated domains. A portion of a typical STM image displaying such undulations is shown in Fig. 2(b). While the (1×1) surface lattice is retained over part of the right-hand side of the imaged area, mild undulations along one of the substrate directions are nonetheless discernible. Moreover, the left-hand portion of the image displays a marked corrugation of this type. Two distinct reconstruction patterns are evident in Fig. 2(b), which were also observed in replicate experiments. The first structure (labeled here I) features prominent single strings of close-packed gold atoms, typically 14 ± 1 atoms long, with each string separated by a distance (14.5 ± 0.5 Å) commensurate with a five-atom gold spacing. A similar "(1×5)" pattern for clean Au(100) in UHV has been observed previously by STM, albeit with poorer resolution [15,16]. The second structure (II) seen in Fig. 2(b) exhibits similar chains of gold, but with a pair of equal intensity strings separated by 4.5–4.6 Å in place of the single strands seen in structure I (*vide infra*). Holding the potential at −0.35 V versus SCE for ca. 10 min or longer yielded surfaces containing predominantly

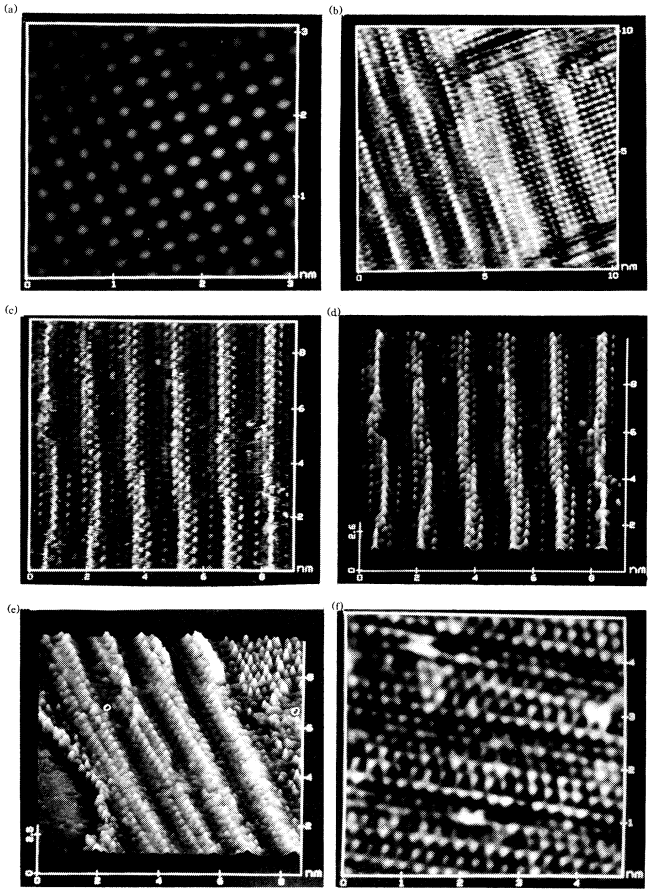

FIG. 2. Typical atomic-resolution STM images obtained for ordered Au(100) in 0.1M $HClO_4$, uncorrected for thermal drift. (a) Filtered 30×30 Å top-view image at electrode potential E =0.2 V vs SCE. Tunneling conditions: Set-point current i_t =20 nA; bias voltage V_b =6 mV. (b) After altering potential (E) to −0.3 V, 10 min later. (c) Well-resolved unfiltered image at E = −0.4 V; i_t =11 nA, V_b =4.3 mV. (d) Height-shaded plot (30° from surface normal) of (c). (e) Height-shaded plot at E = −0.4 V for region containing structure II (see text); i_t =5 nA, V_b =5 mV. (f) Top-view image at E = −0.4 V for rotated domain; i_t =25 nA, V_b =2 mV.

such reconstructed domains, although some (1×1) regions still survived under these conditions. These corrugations were observed in both possible (90°) directions ([0$\bar{1}$1] and [011]) along the square-planar (1×1) lattice. Essentially the same potential-dependent structures were also observed when anodic oxide was not formed and removed voltammetrically prior to the STM data acquisition.

Examination of higher-resolution STM images is informative. Such an image is displayed in the usual top view, and additionally as a "height-shaded" plot (viewed 30° off the surface normal), in Figs. 2(c) and 2(d), respectively. Note that the former is an *unfiltered* image. [The crystal was rotated ca. 15° clockwise for Figs. 2(c) and

2(d) compared with Figs. 2(a) and 2(b).] The domains in the upper portions of Figs. 2(c) and 2(d) display corrugations similar to structure I. Discernible in some parts of this image are five rows of atoms parallel to and in between the most intense strands already noted. The considerably lower intensity of the former rows is an indication of the degree of corrugation; rough estimates (calibrated by the variations in current as the tip is scanned across a monatomic step) suggest that the variations in "height" across the domain strands is ca. 1–2.5 Å.

The parallel strands of atoms are staggered so to form a quasihexagonal close-packed layer. Since six gold atoms are present in the unit-cell dimension normal to the strand direction, the buckled surface layer exhibits a 20% increase in atomic density compared with the unreconstructed substrate. An approximate ball-model representation of structure I as deduced from such images is shown (top and side views) in Fig. 3. Interestingly, this structure is very similar to one likely alternative proposed on the basis of helium diffraction measurements [13] (labeled "model 4" in Ref. [13]). More generally, the real-space observation of these buckled quasihexagonal structures by STM supports the earlier assignment of such configurations from diffraction-based techniques [4,12,13]. In addition, the fourteen-atom strings observed here are consistent with the $c(26\times68)$ unit cell for reconstructed Au(100) as deduced by LEED [12]. This periodicity may result from a slight compression of the interatomic distance along the chains as compared with the underlying substrate.

Figure 2(e) shows a height-shaded surface plot of a surface region (also at -0.35 V versus SCE) where structure II predominates. Besides the appearance of "dual" atomic strands as noted above, this image differs from those for structure I in that it lacks a discernible row of atoms midway between these intensely imaged chains. This and other details of the structure-II images are consistent with a model having a similar symmetry as for structure I, but with the top layer shifted relative to the underlying substrate along the strand direction by one atomic radius (1.45 Å). (This structure, not pictured schematically here, corresponds closely to "model 1" in Fig. 5 of Ref. [13].) Another top-view image of a surface region containing structure II, with the surface corrugations more nearly parallel to the tip scan direction, is shown in Fig. 2(f). Although the furrows appear less marked under these conditions, the hexagonal packing of the reconstructed surface is clearly evident. An additional distinct structure is also discernible in the lower portion of Fig. 2(e). It differs clearly from the domain above it by a ca. 2.0-Å displacement of the top-layer atoms normal to the strand direction. Although many details need to be investigated further, of significance is the likelihood that reconstructed Au(100) surfaces can consist of multiple structurally distinct quasihexagonal domains.

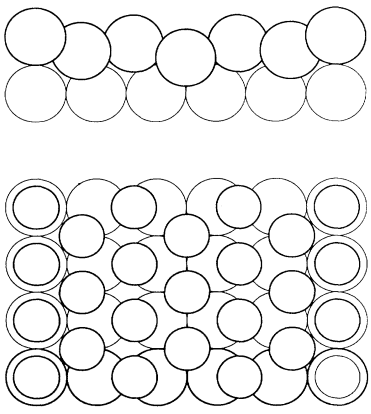

FIG. 3. Suggested ball-model structure (top and side views) of reconstructed Au(100) (structure I), as discerned by STM (note that top-view overlayer Au atoms are drawn smaller for clarity).

Subsequent alteration of the electrode potential back to 0.2 V versus SCE yielded a progressive removal of the reconstructed domains and a return of the dominant (1×1) structure over a ca. 10-min period. The potential-induced reconstruction therefore appears to be largely reversible under these conditions. This observation is qualitatively consistent with information from *in situ* x-ray diffraction [4]. An important unanswered question is the source of the 20% additional gold atoms required to form the reconstructed domains. This issue can, in principle, be addressed in unique fashion by STM. Results so far indicate that reconstruction is triggered preferentially near terrace edges, supporting the notion that the additional gold atoms are supplied from higher step sites.

It is interesting to compare briefly the results herein with pertinent electrochemical data on Au(100) in perchloric acid, which have been discussed previously in the present context [1(a),19]. Cycling the potential slowly between relatively negative and positive potentials, say, from -0.4 to 0.7 V versus SCE in $10mM$ $HClO_4$ [as in Fig. 2(b) of Ref. [19(a)]], yields a significant hysteresis in the differential capacitance-potential (C_d-E) curves. In harmony with the present findings, such data were interpreted in terms of slow reconstruction occurring at negative potentials [1(a)]. Interestingly, the potential of zero charge (PZC), as discerned from the C_d-E minimum in such dilute electrolyte, shifts slightly positive (from ca. 0.05 to 0.1 V versus SCE) as a result of surface reconstruction [20]. This increase in the effective electrochemical "work function" is consistent with the quasihexagonal structure of reconstructed Au(100). [A somewhat larger, ca. 0.15 V, increase in the PZC is seen for unreconstructed Au(111) versus (100) surfaces in dilute perchlorate [21] as expected since the former face exhibits *planar* hexagonal close packing.] It is also worth noting that the Au(100) reconstruction is observed to be ini-

tiated at potentials well below those ($\lesssim 0.2$ V versus SCE) where perchlorate specific adsorption becomes negligible. This suggests that the reconstruction is driven not by potential-induced shifts in adsorption-desportion equilibria, but rather by the surface electrical state, specifically the accumulation of excess electronic charge density at the metal interface.

Overall, then, the present results provide striking evidence of the capabilities of STM for yielding uniquely detailed atomic-level information on reconstruction at electrochemical interfaces. Results in our laboratory indicate that similarly detailed data can also be obtained for a number of other gold crystallographic orientations. Examining the combined effects of electrode potential, time, and also solute adsorption on the metal atomic structure promises to herald a new level of understanding of surface reconstruction on electrochemistry.

We are grateful to Si-Chung Chang and Chris Vitus for experimental assistance. This work is supported by the National Science Foundation and the Office of Naval Research.

---

[a]Permanent address: Laboratoire d'Electrochimie Interfaciale du CNRS, 1 Place A. Briand, 92195 Meudon, France.

[1] (a) A. Hamelin, J. Electroanal. Chem. **142**, 299 (1982); (b) in *Modern Aspects of Electrochemistry,* edited by B. E. Conway, R. E. White, and J. O'M. Bockris (Plenum, New York, 1986), Vol. 16, Chap. 1.

[2] M. S. Zei, G. Lehmpfuhl, and D. M. Kolb, Surf. Sci. **221**, 23 (1989).

[3] A. Friedrich, B. Pettinger, D. M. Kolb, G. Lüpke, R. Steinhoff, and G. Marowsky, Chem. Phys. Lett. **163**, 123 (1989).

[4] B. M. Ocko, J. Wang, A. Davenport, and H. Isaacs, Phys. Rev. Lett. **65**, 1466 (1990).

[5] D. J. Trevor, C. E. D. Chidsey, and D. N. Loiacono, Phys. Rev. Lett. **62**, 929 (1989).

[6] R. J. Nichols, O. M. Magnussen, J. Hotlos, T. Turomey, R. J. Behm, and D. M. Kolb, J. Electroanal. Chem. **290**, 21 (1990).

[7] H. Houbo, S. Sugawara, and K. Itaya, Anal. Chem. **62**, 2424 (1990).

[8] O. M. Magnussen, J. Hotlos, R. J. Nichols, D. M. Kolb, and R. J. Behm, Phys Rev. Lett. **64**, 2929 (1990).

[9] S.-L. Yau, C. M. Vitus, and B. C. Schardt, J. Am. Chem. Soc. **112**, 3677 (1990).

[10] S.-L. Yau, X. Gao, S.-C. Chang, B. C. Schardt, and M. J. Weaver, J. Am. Chem. Soc. (to be published).

[11] C. M. Vitus, S.-C. Chang, B. C. Schardt, and M. J. Weaver, J. Phys. Chem. (to be published).

[12] M. A. Van Hove, R. J. Koestner, P. C. Stair, J. P. Biberian, L. L. Kesmodel, I. Bartos, and G. A. Somorjai, Surf. Sci. **103**, 189 (1981).

[13] K. H. Rieder, T. Engel, R. H. Swendsen, and M. Manninen, Surf. Sci. **127**, 223 (1983).

[14] W. Telieps, M. Mundschau, and E. Bauer, Surf. Sci. **225**, 87 (1990).

[15] G. K. Binnig, H. Rohrer, Ch. Gerber, and E. Stoll, Surf. Sci. **144**, 321 (1984).

[16] Y. Kuk and P. J. Silverman, Appl. Phys. Lett. **48**, 1597 (1986); J. Vac. Sci. Technol. A **8**, 289 (1990); Y. Kuk *et al.*, J. Microsc. **152**, 449 (1988).

[17] A. Hamelin, S. Morin, J. Richer, and J. Lipkowski, J. Electroanal. Chem. **285**, 249 (1990).

[18] S.-C. Chang, S.-L. Yau, B. C. Schardt, and M. J. Weaver, J. Phys. Chem. **95**, 4787 (1991).

[19] (a) F. Silva, M. J. Sottomajor, A. Hamelin, and L. Stoicoviciu, J. Electroanal. Chem. **295**, 301 (1990); (b) A. Hamelin, J. Electroanal. Chem. **255**, 281 (1988).

[20] The larger PZC increase, ca. 0.22 V, reported by D. M. Kolb and J. Schneider [Electrochim. Acta **31**, 929 (1986)] is surprising and in contradiction to the data of Hamelin and co-workers, Ref. [19].

[21] A. Hamelin and M. J. Weaver, J. Electroanal. Chem. **223**, 171 (1987).

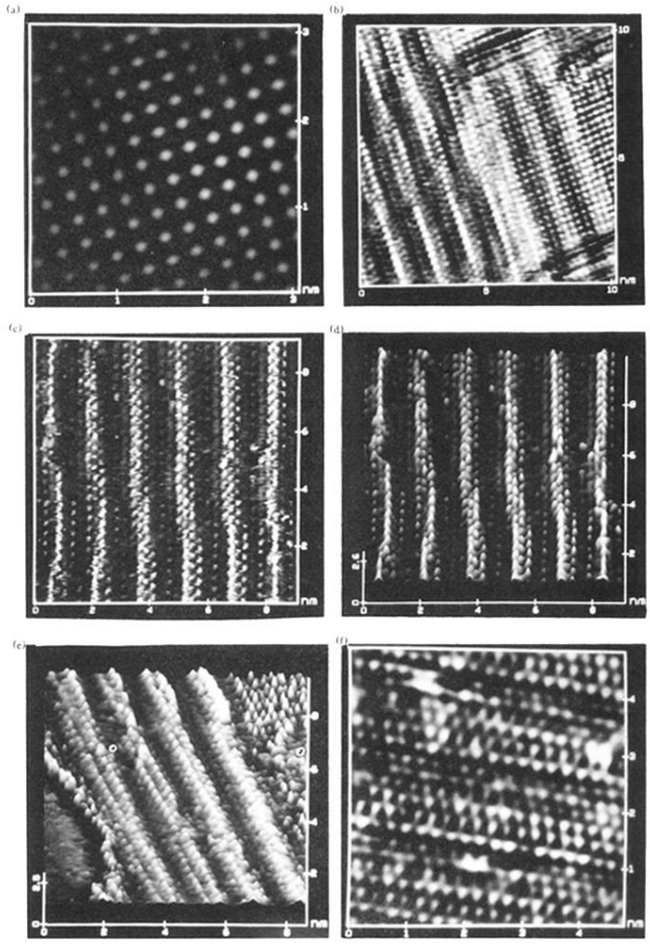

FIG. 2. Typical atomic-resolution STM images obtained for ordered Au(100) in 0.1M $HClO_4$, uncorrected for thermal drift. (a) Filtered 30×30 Å top-view image at electrode potential E=0.2 V vs SCE. Tunneling conditions: Set-point current i_t=20 nA; bias voltage V_b=6 mV. (b) After altering potential (E) to −0.3 V, 10 min later. (c) Well-resolved unfiltered image at E=−0.4 V; i_t=11 nA, V_b=4.3 mV. (d) Height-shaded plot (30° from surface normal) of (c). (e) Height-shaded plot at E=−0.4 V for region containing structure II (see text); i_t=5 nA, V_b=5 mV. (f) Top-view image at E=−0.4 V for rotated domain; i_t=25 nA, V_b=2 mV.